



Stark effect of atomic sodium measured in a hollow cathode plasma by Dopplerfree spectroscopy

F. Moreno, J. M. Alvarez, J. C. Amaré, and E. Bernabeu

Citation: *J. Appl. Phys.* **56**, 1939 (1984); doi: 10.1063/1.334238

View online: <http://dx.doi.org/10.1063/1.334238>

View Table of Contents: <http://jap.aip.org/resource/1/JAPIAU/v56/i7>

Published by the [AIP Publishing LLC](#).

Additional information on *J. Appl. Phys.*

Journal Homepage: <http://jap.aip.org/>

Journal Information: http://jap.aip.org/about/about_the_journal

Top downloads: http://jap.aip.org/features/most_downloaded

Information for Authors: <http://jap.aip.org/authors>

ADVERTISEMENT

Read author interviews in **Bookends**

Stark effect of atomic sodium measured in a hollow cathode plasma by Doppler-free spectroscopy

F. Moreno,^{a)} J. M. Álvarez, J. C. Amaré, and E. Bernabeu^{b)}

Department of Optics, Faculty of Sciences, Zaragoza University, Spain

(Received 28 December 1983; accepted for publication 9 March 1984)

The Stark widths of the 5896-Å ($3^2P_{1/2} \rightarrow 3^2S_{1/2}$) neutral sodium hyperfine lines in the presence of charged perturbers were measured by means of laser saturation spectroscopy. The plasma containing the sodium atoms and the perturbers was generated in a hollow cathode discharge. The Baranger and Brechot theories for the line shape of neutral atom transitions in a plasma has been extended to hyperfine structure and applied to the hyperfine components of sodium D_1 line. The theoretical and experimental results were compared and the electronic density and temperature in the discharge were evaluated.

I. INTRODUCTION

Very high resolution spectroscopic techniques have been used by some experimentalists¹ for studies on a hollow cathode discharge. The relatively high electron density (about 10^{14} cm^{-3}) obtainable by using this type of discharge in comparison with a conventional one (of plane electrodes), without an excessive gas temperature, makes it possible to test experimentally the Stark effect on atomic levels of low energy.

Starting from the theory for Stark effect in plasmas developed by Baranger (1958) and Sahal-Brechot (1969) and with the help of some experimental results from the literature² we have performed in Sec. IV a semiempirical study of the Stark broadening and shift of the D_1 line hyperfine components of atomic sodium in a plasma. The theoretical results have been tested experimentally in a hollow cathode negative glow, by means of the saturated absorption technique to avoid Doppler broadening. The experimental apparatus is described in Sec. II and the experimental values presented in Sec. III are finally discussed in Sec. V by comparison with the theoretical predictions. The results derived and some considerations about the discharge allows us to obtain information on the variation of the electronic temperature T_e and density N_e of the plasma generated.

II. EXPERIMENT

The experimental setup is shown in Fig. 1. An argon ion laser, model 171-09, was employed to pump a tunable dye laser, model 580 A, both from Spectra-Physics. The tunable laser was intensity stabilized, better than 1%, and the internal Fabry-Perot electronically locked to the cavity to avoid mode hopping. So, frequency jitter was minimized to ± 5 MHz.

With the help of an etalon 22.95 cm long, we have performed a calibration of the frequency axis. We shall only consider as representative those points which are separated

by a frequency interval of 10 MHz, and the sweep linearity was estimated better than 3.8%.

The saturating beam was amplitude modulated and the signal coming from the probe beam fed into a lock-in amplifier. The demodulated and filtered signal was stored in a Hewlett-Packard 85-F computer through a digital voltmeter. The piezoelectric elements of the cavity are driven by a triangle-shaped variable voltage. This type of sweep has certain advantages such as the smooth return of the mirrors and consequently the possibility of performing averages of successive measurements in order to optimize the signal-to-noise ratio. The sweep time depends on the time constant (100 ms) of the detection system and on the number of representative points (~ 300) on the signal of frequency range swept; so the sweep time takes the value of 30 sec.

The discharge tube scheme is given in Fig. 2. Pyrex glass was used and the Brewster windows sealed with epoxy. The brass endcaps support the iron electrodes. The anode was an inverted T shape, and the cathode, which had 13-mm i.d. and 30-mm length is continuously refrigerated; a small portion of metallic sodium was located inside the cathode and distributed to the walls by the discharge.

The discharge was fed by an intensity-stabilized power supply through a ballast resistance (725Ω). The currents we have used lie between 100 mA and 200 mA requiring voltages ranging from 340 to 500 V. The discharge was initiated with helium gas at 500 mTorr, and the sodium was fed into the negative glow by sputtering, until a density depending on the discharge intensity is reached.

III. EXPERIMENTAL RESULTS

One of the spectra obtained for the D_1 line with the experimental setup described in Sec. II is shown in Fig. 3. The spectrum has a Gaussian background due to the velocity changing collisions^{3,4} suffered by the sodium atoms during their interaction with the laser beam. On the same figure we can see that the $D_1 (i +)$ line hyperfine components are resolved; but in the $D_1 (i -)$ line only the more intense component ($3^2P_{1/2}, F = 2 \rightarrow 3^2S_{1/2}, F = 1$) appears while the other component ($3^2P_{1/2}, F = 1 \rightarrow 3^2S_{1/2}, F = 1$) is very weak and it is masked by a crossover signal. On the other hand, the

^{a)} Present address: Department of Optics, Faculty of Sciences, Santander University, Santander, Spain.

^{b)} Present address: Department of Optics, Faculty of Sciences, Barcelona University, Bellaterra, Barcelona, Spain.

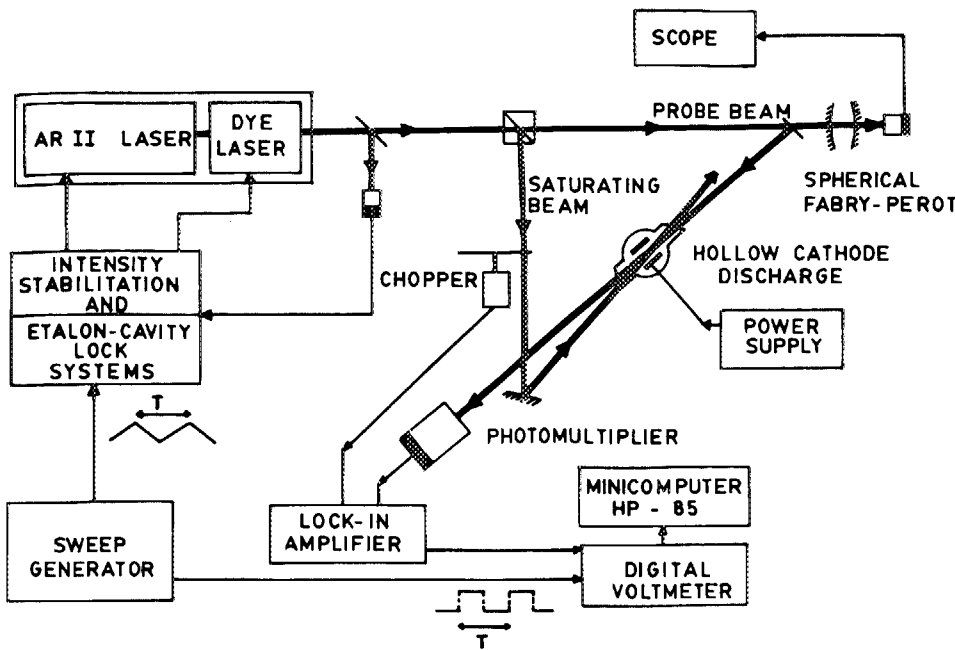


FIG. 1. Experimental systems.

assymetry of the D_1 line background is due to the inverted crossover signal that appears between these transitions.

From the theories recently developed by Berman⁴, which take into account the effect of the velocity changing collisions on the emitted line shape (in our case sodium D_1 lines), we were able to obtain the Stark widths of the transitions under study. To do this, the theoretical signals were fitted to the experimental ones. [The result of this fitting is also shown in Fig. 3 (dotted line)]. From this fitting we obtained the width of the Lorentzian part of the spectrum. To obtain the contribution of the Stark effect we have subtracted the contributions coming from the natural widths (~ 62 MHz), phase-changing collisions with helium atoms (~ 7 MHz) at 500 mTorr,⁵ power broadening (~ 40 MHz), and residual Doppler broadening due to the nonparallelism between saturating and probe beams.

Figure 4 shows the dependence of the measured Stark width on the discharge current in the range of interest. The four hyperfine components have a similar behavior. The contribution of mechanisms other than the Stark effect on the signal has been tested in a saturated absorption experiment in pure sodium.

IV. THEORY

We have calculated the effect of the electron and ion collisions on the D_1 line hyperfine components of sodium atoms with the help of the theories developed.^{6,7} Taking into account the validity of the impact and classical path approximations, we have obtained the Stark broadening and shift of the transition between atomic hyperfine levels $|F_i\rangle$ and $|F_f\rangle$ of an alkali atom. It can be expressed in the isolated line approximation as follows:

$$w + id = \frac{4\pi}{3} N_e \int_0^\infty \frac{f(v)dv}{v} \sum_{F_i, F_f} |\langle F_i' | r | F_i, f \rangle|^2 Q_{i, f} W_{i, f}^{(1)} \times [a(Z'_{i, f \min}) + ib(Z'_{i, f \min})] + \frac{4\pi}{15} \times N_e \int_0^\infty \frac{f(v)dv}{v^3} \sum_{F_i, F_f} |\langle F_i' | r^2 | F_i, f \rangle|^2 \times Q_{i, f} W_{i, f}^{(2)} \omega_{i, f}^2 [a_q(Z'_{i, f \min}) + ib_q(Z'_{i, f \min})]. \quad (1)$$

In Eq. (1), we have taken $\hbar = m_e = a_0 = 1$, and

$$Q_{i, f} = (2F_i' + 1)(2J_i, f + 1) \times (2J_i' + 1)(2L_i, f + 1)(2L_i', f + 1),$$

$$W_{i, f}^{(n)} = \begin{Bmatrix} J_i', f & F_i', f & I \\ F_i, f & J_i, f & n \end{Bmatrix} \begin{Bmatrix} L_i', f & J_i', f & S \\ J_i, f & L_i, f & n \end{Bmatrix} \begin{pmatrix} L_i', f & n & L_i, f \\ 0 & 0 & 0 \end{pmatrix}^2,$$

$Z'_{i, f \min} = \omega_{i, f} b_{\min}/v$, b_{\min} being the limit impact parameter and $f(v)$ is the perturbing atoms velocity distribution. The functions $a(Z)$, $b(Z)$, $a_q(Z)$, and $b_q(Z)$ result from the average over the perturbing atoms impact parameters and integration over time.^{8,9} If the impact parameter is less than b_{\min} , the collision should be considered as a strong collision and for them the time dependent perturbation theory cannot be used. The contribution of strong collisions to the Stark

width has a value given by

$$W_{sc} = \pi N_e \int_0^\infty v f(v) b_{\min} dv.$$

The effect of the presence of ions has a negligible contribution in comparison with that of the electrons (about 1%) and as a consequence of this we can expect a Lorentzian

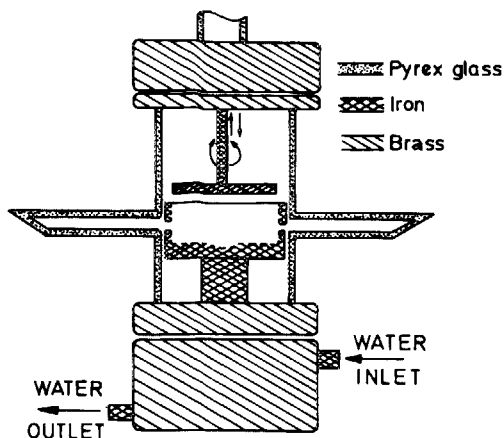


FIG. 2. Discharge tube scheme.

shape for the spectrum of every hyperfine transition of the D_1 line. The Stark width and shift are given by Eq. (1) plus the contribution due to strong collisions.

In order to test the validity of the approximations used to obtain Eq. (1), a previous diagnostic of plasma has been performed from the intensity ratio between the 4686-Å He-II line and the 5876-Å He-I line. We have estimated the values of 10^{14} cm^{-3} for the electronic density and $7 \times 10^4 \text{ K}$ for the electronic temperature. With this value the impact approximation is justified because the collision frequency is

$$\nu \sim 10 \text{ MHz} \ll \tau_c^{-1} \sim 10^6 \text{ MHz},$$

τ_c being the collision time with an electron. The classical path approximation is also valid because the De Broglie wavelength associated with the electron λ_e is less than the

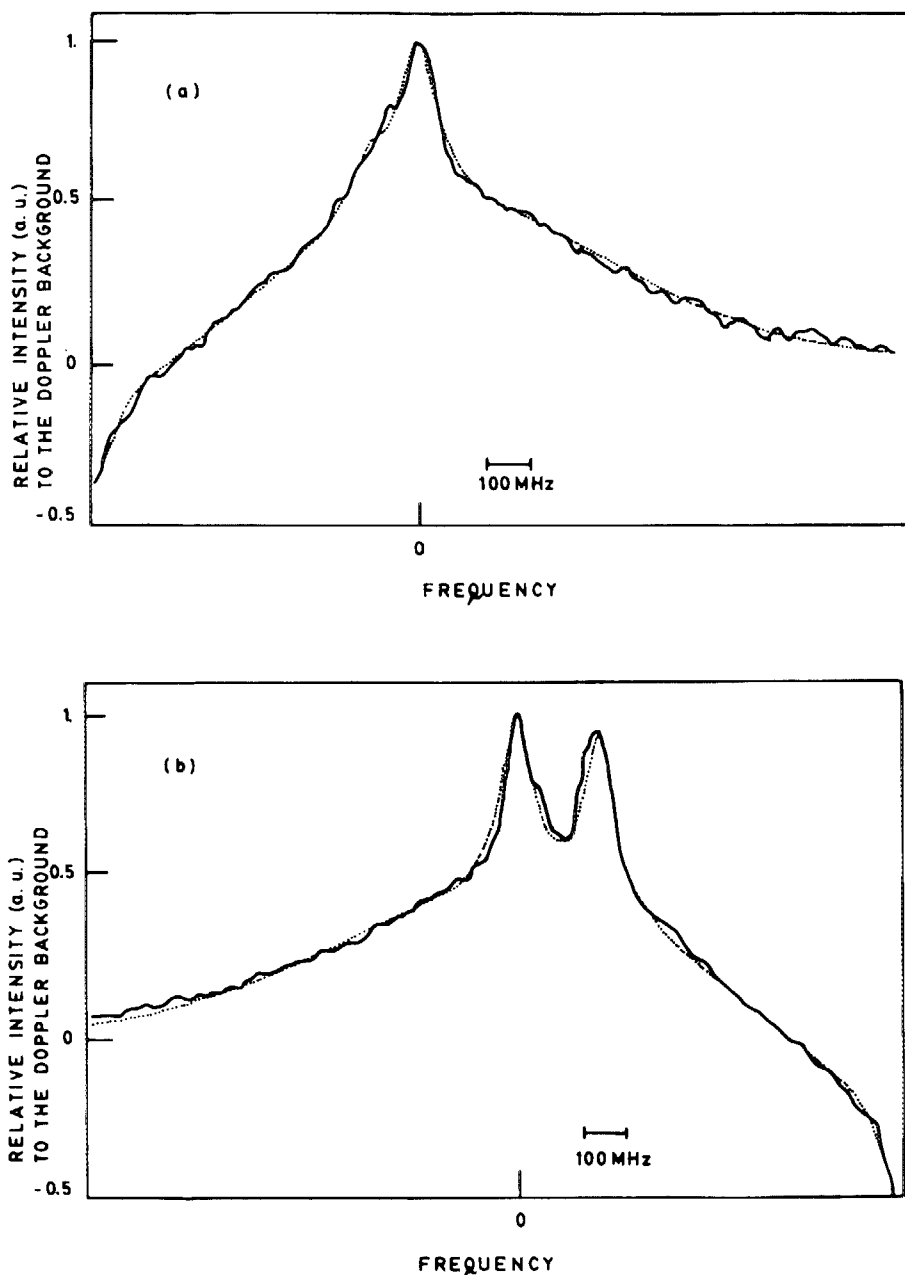


FIG. 3. Measured spectra of the D_1 line (continuous line) and theoretical fitting (broken line). Discharge current was 100 mA. (a) $D_1(i-)$ component. (b) $D_1(i+)$ component.

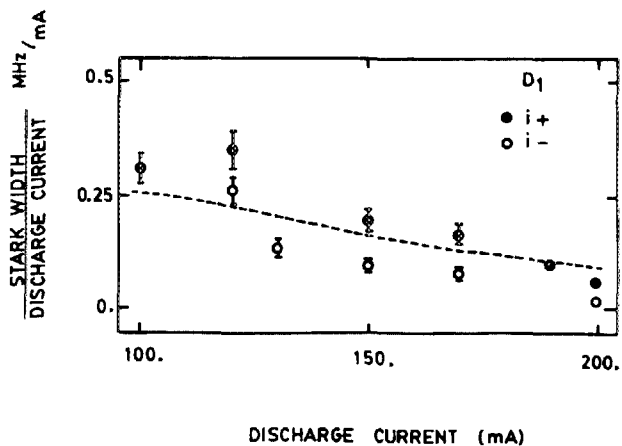


FIG. 4. Measured Stark width and theoretical fitted evolution (broken line).

average impact parameter

$$\bar{b} \sim 10^3 \text{ \AA} \gg \lambda_e \sim 1 \text{ \AA}.$$

For the D_1 line hyperfine components we can assume the isolated line approximation since the hyperfine splitting of $3^2P_{1/2}$ (192 MHz) and $3^2S_{1/2}$ (1772 MHz) are one and two orders of magnitude greater than the estimated Stark widths. In Fig. 5, the calculated Stark width is plotted versus the electronic temperature. (T_e and N_e being given in the range of interest). The evolution of the Stark width has been fitted to the function

$$W(T_e, N_e) = \frac{N_e}{10^{14}} [85.24 - 63.2 \exp(-T_e/28.3 \times 10^3)], \quad (2)$$

where W must be expressed in MHz, N_e in cm^{-3} , and T_e in $^{\circ}\text{K}$. This analytic form gives a good fitting of the theoretical evolution as it can be seen in Fig. 5 and it will be useful to study the dependence of N_e and T_e on the discharge current.

V. DISCUSSION

Experimentally it is observed that the Stark width and the voltage difference between the electrodes decreases when the current in the discharge is increases. From this behavior we can conclude that an increase of the current produces a

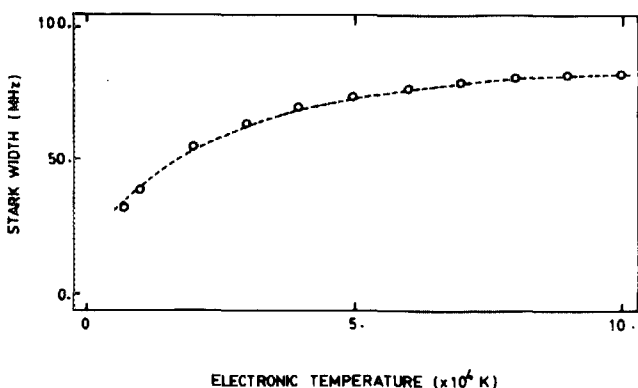


FIG. 5. Theoretical evolution of the Stark width and fitting to $W(T_e, N_e)$ (continuous line).

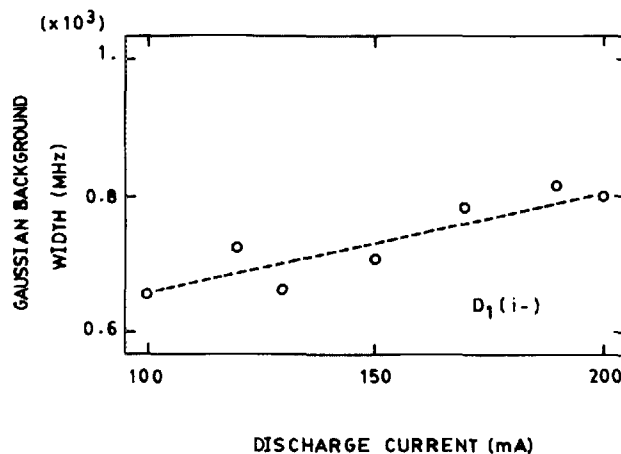


FIG. 6. Evolution of the Gaussian background width vs the current discharge. Lineal fitting (broken line).

decrease of the electronic temperature.

On the other hand, the optical density measurement on the D_1 line gives for variation of the sodium density a dependence on the current intensity I of the discharge given by

$$n_{\text{Na}}(I) = 3.6 \times 10^{10} \exp(0.025I),$$

where n_{Na} is given in cm^{-3} and I in mA.

The electronic temperature T_e can be expressed as

$$T_e = T_g + \frac{T}{[\text{coll}(\text{He})] + [\text{coll}(\text{Na})]},$$

T_g being the gas temperature. The second term informs on the energy excess of the electrons accelerated from the cathode walls into the negative glow by the electronic field of the dark space and braked by collisions with helium and sodium atoms. On the other hand, from the evolution of the Gaussian width of the background as a function of the intensity current, Fig. 6, we can extract the quadratic law for the gas temperature in $^{\circ}\text{K}$

$$T_g = 9.80 \times 10^{-4} (2.4I + 430)^2.$$

So, the expression for the electronic temperature T_e as a

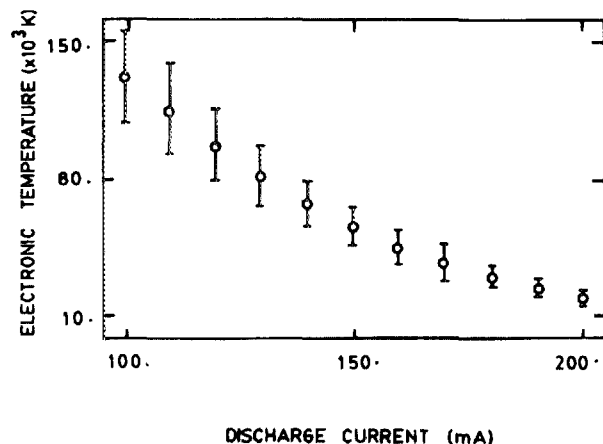


FIG. 7. Calculated evolution of the electronic density N_e vs the discharge current intensity I .

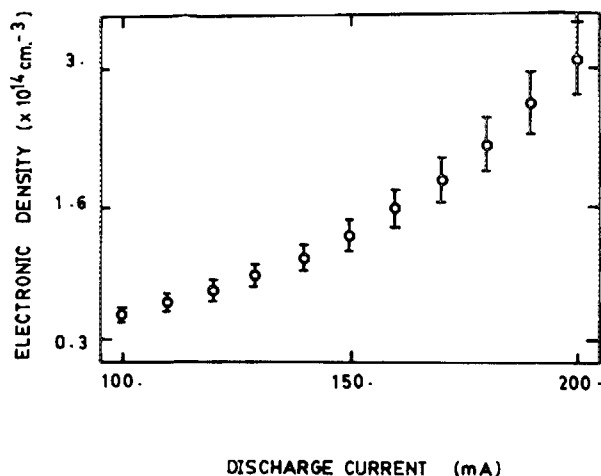


FIG. 8. Calculated evolution of the electronic temperature T_e vs the discharge current intensity I .

function of I can be written as follows

$$T_e = 9.80 \times 10^{-4} (2.4I + 430)^2 + \frac{1}{B + C \exp(0.025I)}, \quad (3)$$

where B and C are parameters related to the total collision cross sections between the electron and helium and sodium atoms, respectively.

The geometry of hollow cathode in our discharge tube allows us to write

$$N_e T_e^{1/2} = \alpha I, \quad (4)$$

α being a parameter related to the geometry and kinetic of electrons. From Eq. (3), Eq. (4), and the expression (2) is obtainable the theoretical evolution of $W(T_e, N_e)$ as a function of the current intensity, I . The fit of the expression obtained to the experimental results (plotted in Fig. 4) leads to the values of the parameters B , C , and α . The substitution of these values into Eqs. (3) and (4) leads to the evolution of N_e and T_e on I . They are plotted in Figs. 7 and 8, respectively. In these plots we can see that the electronic density increases from $3.05 \times 10^{13} \text{ cm}^{-3}$ at 100 mA to $3.69 \times 10^{14} \text{ cm}^{-3}$ at 200 mA; under the same conditions the electronic temperature decreases from $15 \times 10^4 \text{ K}$ to $2.3 \times 10^4 \text{ K}$. The estimated error in the determination of N_e is better than 12% and better than 20% in that of T_e .

¹J. E. Lawler, A. Siegel, B. Conillard, and T. W. Hänsch, *J. Appl. Phys.* **52**, 4375 (1981).

²N. Konjevic and J. R. Roberts, *J. Phys. Chem. Ref. Data* **5**, 209 (1976).

³C. Brechignac, R. Vetter, and P. R. Bermann, *Phys. Rev. A* **12**, 1609 (1978).

⁴P. R. Bermann, *Phys. Rev. A* **25**, 2550 (1982).

⁵E. W. Weber and K. Jungmann, presented at the European Conference on Atomic Physics, Heidelberg, Germany (1981), edited by J. Kowalski, G. Zu Putlidz, and H. G. Weber, Vol. 5A, pp. 521-522.

⁶M. Baranger, *Phys. Rev.* **111**, 481 (1958); **111**, 494 (1958); **112**, 855 (1958).

⁷S. Sahal-Brechot, *Astron. Astrophys.* **1**, 91 (1969).

⁸J. Cooper and G. K. Oertel, *Phys. Rev.* **180**, 286 (1969).

⁹S. Krasfeld, *Phys. Lett. A* **32**, 26 (1970).